Available online at www.sciencedirect.com
SCIENCE DIRECT®
Journal of Nuclear Materials 320 (2003) 258–264
journal of nuclear materials
www.elsevier.com/locate/jnucmat

Standard molar Gibbs free energy of formation of PbO(s) over a wide temperature range from EMF measurements

Rajesh Ganesan [a], T. Gnanasekaran [a,*], Raman S. Srinivasa [b]

[a] Sodium Chemistry Section, Materials Chemistry Division, Indira Gandhi Centre for Atomic Research, Kalpakkam 603 102, India
[b] Department of Metallurgical Engineering and Materials Science, Indian Institute of Technology Bombay, Mumbai 400 076, India

Received 30 May 2002; accepted 5 March 2003

Abstract

The EMF of the following galvanic cells,

$$\text{Kanthal, Re, Pb, PbO} \mid \text{CSZ} \mid \text{O}_2\ (1\ \text{atm.}), \text{Pt} \qquad \text{(Cell(I))}$$

$$\text{Kanthal, Re, Pb, PbO} \mid \text{CSZ} \mid \text{O}_2(1\ \text{atm.}), \text{RuO}_2, \text{Pt} \qquad \text{(Cell(II))}$$

were measured as a function of temperature. With O_2 (1 atm.), RuO_2 as the reference electrode, measurements were possible at low temperatures close to the melting point of Pb. Standard Gibbs energy of formation, $\Delta_f G^0_m\langle\beta\text{-PbO}\rangle$ was calculated from the emf measurements made over a wide range of temperature (612–1111 K) and is given by the expression: $\Delta_f G^0_m\langle\beta\text{-PbO}\rangle \pm 0.10\ \text{kJ} = -218.98 + 0.09963T$. A third law treatment of the data yielded a value of $-218.08 \pm 0.07\ \text{kJ mol}^{-1}$ for the enthalpy of formation of PbO(s) at 298.15 K, $\Delta_f H^0_m\langle\beta\text{-PbO}\rangle$ which is in excellent agreement with second law estimate of $-218.07 \pm 0.07\ \text{kJ mol}^{-1}$.

PACS: 05.70.−a

1. Introduction

Liquid lead and lead–bismuth eutectic (LBE) alloys are currently being explored for service as coolant in nuclear reactors and accelerator driven systems [1]. Liquid lithium–lead is considered as a candidate material as tritium breeder in fusion reactors [2]. Owing to its relatively low chemical reactivity, LBE alloy is being considered as an alternative to liquid sodium coolant in fast breeder reactors. This eutectic alloy, having a composition of 44.1 at.% Pb in Bi and an eutectic temperature of 125 °C [3], has been extensively used as coolant in compact nuclear reactors in submarines in Russia [4]. Though pure Pb–Bi coolant is corrosive towards structural steels, a protective oxide layer that prevents this corrosion can be formed over the structural steels by suitable control of oxygen concentration in this alloy [5]. Oxygen needed for this purpose is maintained in the coolant by the use of a hot column in the coolant circuit loaded with a solid solution of lead and bismuth oxide [6]. The extent of dissolution of this oxide and maintenance of the dissolved oxygen level in the LBE are dictated by the thermochemical properties of the oxides involved and the kinetics of their dissolution.

A compilation of the available phase equilibria and thermochemical data on Pb–O system was reported by Wriedt in 1988 [7]. Risold et al. have recently reported a thermodynamic description of this system based on the literature data [8]. Among the oxides of lead, the monoxide PbO(s) coexists with liquid lead [3]. PbO(s) has two crystallographic modifications: (i) red α-PbO

* Corresponding author. Tel.: +91-4114 280098; fax: +91-4114 280065.
E-mail address: gnani@igcar.ernet.in (T. Gnanasekaran).

0022-3115/03/$ - see front matter © 2003 Elsevier B.V. All rights reserved.
doi:10.1016/S0022-3115(03)00191-0

which is a low temperature phase and (ii) yellow β-PbO stable at high temperatures. The transformation between these two phases is reported to be sluggish [8]. The transformation temperature and the enthalpy of transition have not yet been unequivocally determined. Based on the reported data in literature, a transition temperature of 762 K has been recommended in thermochemical compilations by Knacke et al. [9] and Chase et al. [10], and by Risold et al. [8]. The values of enthalpy of transition reported in literature [7,8] are low but widely different. Recommended values by Chase et al. [10], Knacke et al. [9], and Risold et al. [8] are 167 ± 293, 715 and 1027 $J\,mol^{-1}$, respectively.

Various investigators have measured Gibbs energy of formation of PbO(s) using solid oxide electrolyte emf cells [11–23] and the cells employed in these works are listed in Table 1. Measurements of these data at temperatures lower than 750 K had been limited and this was mainly due to the sluggish response of the reference electrodes employed – a metal/metal oxide pair or oxygen/air reference with porous platinum electrode, at low temperatures. When metal/metal oxide pair is used as the reference electrode, the uncertainties in the values of free energy of formation of the reference metal oxide would add up to the uncertainties in the derived values and hence use of gas reference electrode of precise oxygen partial pressure is generally preferred [24]. Use of electrically conducting oxides as electrode with oxygen/air reference system has been known to extend the utility of the zirconia based emf cells to temperatures below 750 K [25,26]. Bannister had used $Pt + (U_{0.38}Sc_{0.62})O_{2\pm x}$ as the electrode material with air as reference and measured Gibbs energy of formation of PbO(s) down to 645 K [22]. Periaswami et al. have shown that zirconia based oxygen gauges can be successfully employed at low temperatures using RuO_2 as the electrode material in place of conventional porous platinum [27]. In the present work, a cell using oxygen gas as reference with RuO_2 as electrode material was employed and Gibbs energy of formation of PbO(s) was determined down to 612 K. Measurements were also carried out using conventional porous platinum as the electrode material.

2. Experimental

The electrode materials used were granular Pb (purity 99.99% by mass, M/s. Johnson Matthey Inc., USA) and PbO powder (purity 99.999% by mass, M/s. Aldrich Chem. Co., USA). One end closed calcia stabilised zirconia solid electrolyte tubes with flat bottom (11 m/o $CaO–ZrO_2$; 13 mm OD, 9 mm ID and 250 mm long) supplied by M/s. Nikkato Corporation, Japan were used for constructing the galvanic cells which are given below:

$$\text{Kanthal, Re, Pb, PbO} \mid \text{CSZ} \mid \text{O}_2\ (1\ \text{atm.}), \text{Pt}, \qquad \text{(Cell-I)}$$

$$\text{Kanthal, Re, Pb, PbO} \mid \text{CSZ} \mid \text{O}_2(1\ \text{atm.}), \text{RuO}_2, \text{Pt}. \qquad \text{(Cell-II)}$$

The schematics of the experimental assemblies used are shown in Fig. 1. For Cell-I, platinum coating over the inner bottom end of electrolyte tube was achieved by applying platinum paste (M/s. Eltecks Corporation, India) over the desired part and heating it at 800 °C for 5 h in air. This resulted in a uniform and porous platinum film over the electrolyte. A Pt wire co-fired with the platinum paste served as the electrical lead. A

Table 1
$\Delta_f G^0_m$ of PbO(s) derived from EMF experiments

S. no.	$\Delta_f G^0_m = -A + BT$ ($kJ\,mol^{-1}$)	EMF cell	Temp. range (K)	$\Delta_f G^0_m\langle PbO\rangle$ ($kJ\,mol^{-1}$)			Ref.
				700 K	900 K	1100 K	
1	$-218.98 + 0.09963T$	Pb, PbO|CSZ|O_2	612–1111	−149.24	−129.31	−109.39	This work
2	$-219.37 + 0.10092T$	Pb, PbO|MSZ|Ni, NiO Pb, PbO|MSZ|Cu, Cu_2 O	720–1070	−148.73[a]	−128.54	−108.36[a]	[11]
3	$-218.07 + 0.09820T$	Pb, PbO|CSZ| Ni, NiO	773–1159	−149.33[a]	−129.69	−110.05	[12]
4	$-215.06 + 0.09639T$	Pb, PbO|CSZ| O_2	772–1160	−147.59[a]	−128.31	−109.03	[13]
5	$-218.10 + 0.09889T$	Pb, PbO|CSZ|Ni, NiO	748–1130	−148.88[a]	−129.10	−109.32	[14]
6	$-215.06 + 0.09623T$	Pb, PbO|CSZ|O_2	1023–1170	−147.70[a]	−128.45[a]	−109.21	[15]
7	$-214.10 + 0.09414T$	Pb, PbO|CSZ|Fe, FeO	993–1159	−148.20[a]	−129.37[a]	−110.55	[16]
8	$-214.66 + 0.09565T$	Pb, PbO|CSZ|?	865–1159	−147.70[a]	−128.57	−109.44	[17]
9	$-215.00 + 0.09728T$	Pb, PbO|CSZ|Ni, NiO	923–1152	−146.90[a]	−127.45[a]	−107.99	[18]
10	$-216.61 + 0.09803T$	Pb, PbO|CSZ|O_2	1023–1143	−147.99[a]	−128.38[a]	−108.78	[19]
11	$-215.23 + 0.09654T$	Pb, PbO|CSZ|O_2	1073–1145	−147.65[a]	−128.34[a]	−109.04	[20]
12	$-216.00 + 0.09740T$	Pb, PbO|CSZ or YSZ|O_2	673–1160	−147.82	−128.34	−108.86	[21]
13	$-220.01 + 0.10091T$	Pb, PbO|YSZ|O_2	645–977	−149.37	−129.19	−109.01[a]	[22]
14	$-212.64 + 0.09254T$	Pb, PbO|CSZ|O_2	767–901	−147.86[a]	−129.35	−110.85[a]	[23]

[a] Extrapolated data.

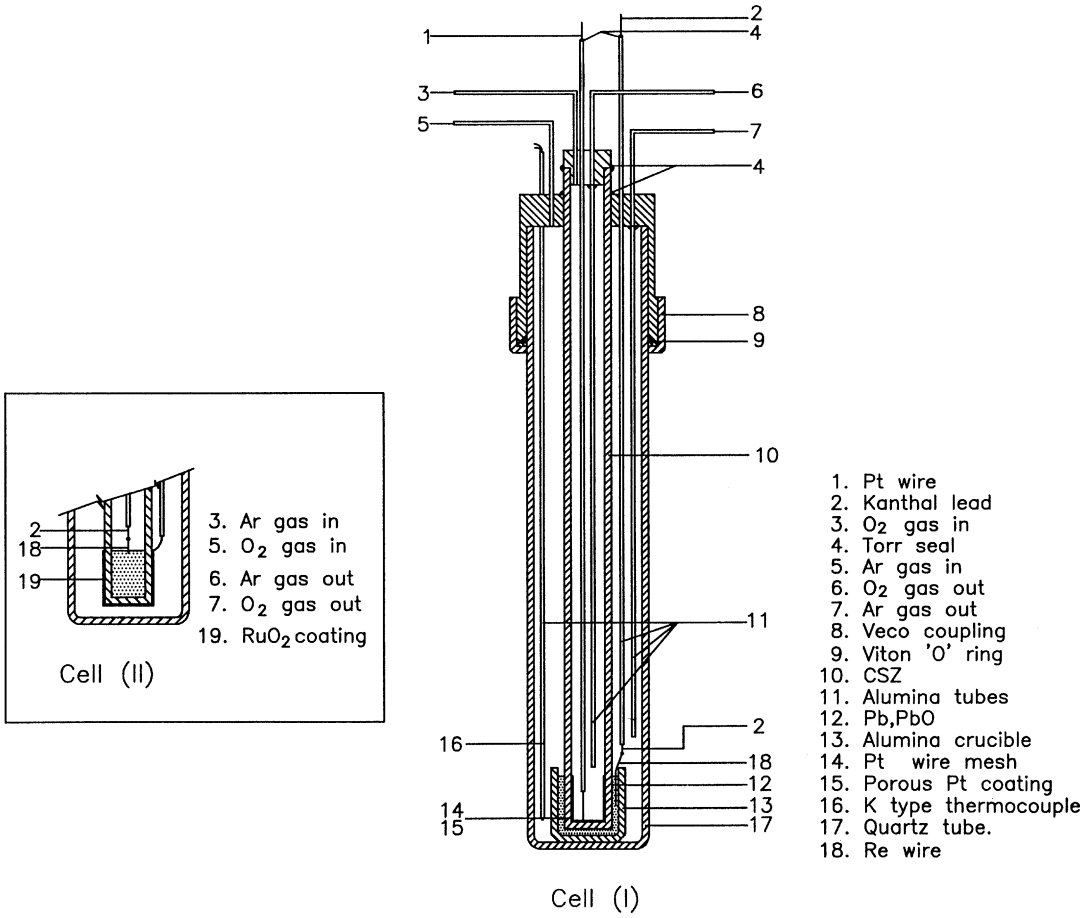

Fig. 1. Schematics of the emf cells I and II.

mixture of Pb and PbO (25:1 by mass) was taken in an alumina crucible into which the solid electrolyte tube was inserted. For Cell-II, RuO_2 coating was achieved by painting a solution of $RuCl_3$ (purity 99.99% by mass, M/s. Koch-Light, England) in acetone over the outer side of closed end of the electrolyte and heating it at 850 °C for 5 h in air. This process resulted in a shining blue black and electrically conducting coating of RuO_2 over the electrolyte surface. A platinum wire tied over this RuO_2 coating served as electrical lead. In Cell-II, the Pb/PbO mixture was taken inside the solid electrolyte tube. Re in the form of a filament (purity 99.999% by mass, M/s. Johnson Matthey Inc., USA) spot welded to a Kanthal wire was used as electrical lead for the Pb/PbO electrode. Rhenium was chosen as the electrical contact because of its chemical compatibility with this system [3]. The cell was housed in a quartz tube using an O-ring seal. This arrangement had provisions for measuring cell temperature and for flowing high purity argon and oxygen gases through Pb/PbO electrode and reference compartments, respectively. The cell assembly was placed in the constant temperature zone of the furnace. Additionally a 100 mm long, hollow cylindrical stainless steel block was placed in the constant temperature zone of the furnace to further enhance the uniformity of the temperature in the zone and the cell temperature could be controlled within ± 0.2 K using a PID temperature controller. The stainless steel block was grounded to avoid any ac pickup by emf signal. The cell temperature was measured using a K-type thermocouple and this thermocouple was calibrated prior to actual experiments against a standard calibrated thermocouple supplied by National Physical Laboratories, India. The cell emf was measured using a high impedance electrometer (input impedance $> 10^{14}$ Ω, Keithley model-617) and the temperature was measured using a multimeter (Hewlett-Packard model-34401A). The data were acquired through an IBM PC using GPIB interface.

Measurements were made in the temperature range 731–1111 K for Cell-I and in the range of 612–1009 K for Cell-II. With Cell-II, the measurements at high temperatures, above 800 K were carried out at a few

Table 2
Experimental EMF results for Cell-I Kanthal, Re, Pb, PbO | CSZ | O_2 (1 atm.), Pt

T (K)	E (mV)
768.2[h1]	738.1
868.9[h1]	685.8
967.9[h1]	634.8
770.8[r1]	736.9
871.4[r1]	684.6
971.4[c1]	632.9
922.0[c1]	658.4
824.4[c1]	708.9
786.1[c1]	729.2
836.8[h2]	702.6
887.0[h2]	676.5
937.4[h2]	650.4
987.8[h2]	624.6
1037.7[h2]	599.1
1087.6[h2]	574.0
1058.7[h2]	588.4
1008.5[c2]	613.9
952.9[c2]	642.4
907.6[c2]	665.7
851.5[c2]	694.4
801.7[c2]	720.5
751.4[c2]	746.4
1097.5[c3]	569.5
1072.6[c3]	581.8
1047.5[c3]	594.4
1022.4[c3]	607.0
997.4[c3]	619.7
962.0[c3]	637.8
860.9[c3]	690.0
811.2[c3]	715.4
871.6[r2]	684.8
781.4[r2]	731.3
882.0[h3]	679.5
931.8[h3]	653.7
1031.7[h3]	602.3
1111.0[r3]	561.5
731.0[a,r3]	757.5

[h1]Heating cycle 1; [h2]Heating cycle 2; [h3]Heating cycle 3.
[c1]Cooling cycle 1; [c1]Cooling cycle 2; [c1]Cooling cycle 3.
[r1]Random measurements set 1; [r2]Random measurements set 2; [r3]Random measurements set 3.
[a] Equilibrated for 16 h.

temperatures only since loss of RuO_2 by evaporation during prolonged operation at high temperatures is known [27]. The thermo emf due to dissimilar electrical leads viz., Kanthal [1] – platinum couple was measured and corrected for in cell emf. Measurements were carried out for several heating, cooling and in random cycles. Generally the emf values became steady within 10 min after attaining a stable cell temperature. The readings were taken when the stability of the cell emf values were within $\pm 5 \times 10^{-5}$ V and the stability of the output was monitored at least for 30 min when temperatutes were above 950 K and for at least 3–4 h when the temperatures were below 950 K before making the measurements. Reproducibility of the cell emf was checked by micro-polarisation and thermal cycling.

Taking into account of the sluggish nature of β-PbO to α-PbO transition, emf measurements at temperatures below 762 K were made after prolonged equilibrations also (≈15–48 h, see Tables 2 and 3). With a view to characterise the phase that coexists with liquid lead during these emf measurements at low temperatures, additional equilibration experiments were carried out. For these equilibrations, Pb(s) and PbO(s) were taken with mass ratios of 5:1 and 7:1 in alumina crucibles, placed in quartz tubes and maintained at 725 K for 115 h with a flow of high purity argon over the samples. The equilibrated samples were then cooled and analysed with XRD to identify the phases present.

3. Results and discussion

The cell reaction can be represented as

$$\mathrm{Pb(l)} + 1/2\,\mathrm{O_2(g, 1\ atm.)} \Longleftrightarrow \mathrm{PbO(s)}. \quad (1)$$

Table 3
Experimental EMF results for Cell-II Kanthal, Re, Pb, PbO | CSZ | O_2 (1 atm.), RuO_2, Pt

T (K)	E (mV)
860.3[c1]	689.9
811.2[c1]	715.5
760.5[c1]	741.9
711.3[a,c1]	767.8
661.8[b,c1]	793.8
612.1[c1]	819.2
637.3[h1]	806.5
689.1[c,h1]	779.5
738.4[h1]	753.7
787.9[h1]	727.8
652.1[r1]	798.6
649.6[h2]	799.8
699.3[b,h2]	774.1
748.2[h2]	748.5
797.7[h2]	722.6
834.6[h2]	703.4
1009.3[h2]	613.6

[h1]Heating cycle 1; [h2]Heating cycle 2.
[c1]Cooling cycle 1.
[r1]Random measurements set 1.
[a] Equilibrated for 16 h.
[b] Equilibrated for 15 h.
[c] Equilibrated for 48 h.

[1] As the junction between Kanthal and Re was present in the constant temperature zone of the furnace along with the sensor head, the thermo emf due to Kanthal-Re need not be considered.

The values of EMF measured from Cell-I and Cell-II are given in Tables 2 and 3, respectively. Fig. 2 shows the variation of the cell emf with temperature. It can be seen from the plot that the data obtained from both the cells are in very good agreement with each other. It is also to be noticed that the transition from α-PbO to β-PbO could not be detected in the present measurements although measurements in the present study covered a wider temperature range near the reported transition temperature. Similar observations have also been made by Alcock and Belford [11], Jacob and Jeffes [14] and Bannister [22] during their measurements. XRD analysis of the products obtained after equilibration at 725 K for 115 h clearly indicated the presence of high temperature phase of lead oxide (β-PbO) only. This is in agreement with the observation of White et al. [28] who had reported the retention of the high temperature phase even after heating it at 573 K for ≈9 days. Hence the measured emf values of the present study correspond to the β-PbO(s)–Pb(l) equilibrium throughout the studied temperature range. Linear least squares fitted expression of the emf data from both the cells is given below:

$$E \pm 0.0005\ \mathrm{V} = 1.1348 - 5.163 \times 10^{-4} T\ (\mathrm{K}) \quad T: 612\text{–}1111\ \mathrm{K}, \tag{2}$$

where the error quoted is the standard deviation from the straight line. Using this emf values, the standard Gibbs energy of formation of β-PbO(s) is calculated using the Nernst equation and is given by

$$\Delta_f G^0_m(T) \pm 0.10\ \mathrm{kJ} = -218.98 + 0.09963T\ (\mathrm{K}) \quad T: 612\text{–}1111\ \mathrm{K}. \tag{3}$$

To assess the existence of any systematic errors and their temperature dependency, third law treatment of the data was made. Using the free energy function of β-PbO(s) listed in Chase et al. [10], $\Delta_f H^0_m$(β-PbO, s, 298.15 K) was calculated for each experimental data point and the values obtained are shown in Fig. 3. As shown in the figure, the derived values of $\Delta_f H^0_m$(β-PbO, s, 298.15 K) are only randomly scattered within the quoted standard deviation indicating the absence of any systematic errors. The second law estimate of $\Delta_f H^0_m$(β-PbO, s, 298.15 K) was obtained by slope method. Using the mean enthalpy of reaction obtained from Eq. (3) and enthalpy increment data listed in Chase et al. [10], $\Delta_f H^0_m$(β-PbO, s, 298.15 K) was calculated as -218.07 ± 0.07 kJ mol^{-1}. This matches exactly with the mean value of third law estimate of -218.08 ± 0.07 kJ mol^{-1}. Both are in excellent agreement with the value of -218.06 ± 0.63 kJ mol^{-1} compiled by Chase et al. [10].

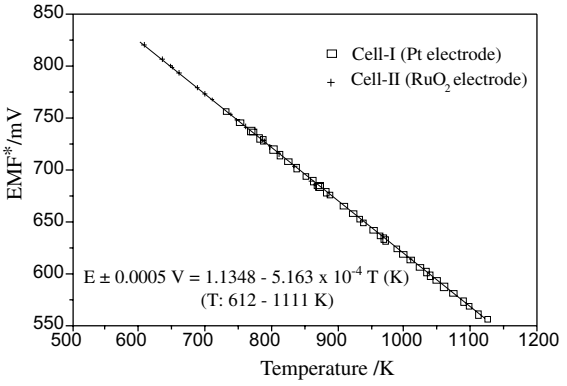

Fig. 2. Variation of EMF as a function of temperature from Cell-I and Cell-II. (* Thermo emf corrected).

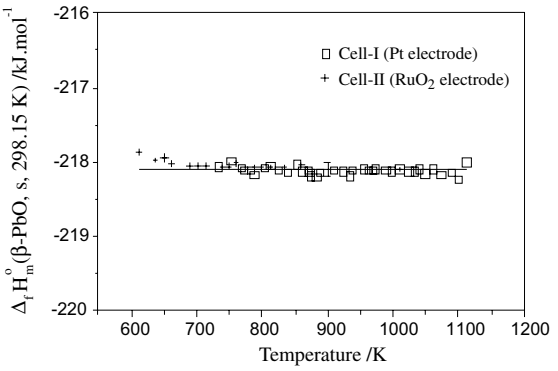

Fig. 3. $\Delta_f H^0_m$(β-PbO, s, 298.15 K) determined by third law computations from the Gibbs energy data.

The data on $\Delta_f G^0_m\langle \mathrm{PbO} \rangle$ from this work as well as those reported in literature are shown in Table 1. With a view to compare them, the difference between free energy values reported in each work and those listed in Chase et al. [10] are plotted in Fig. 4 as a function of temperature up to the melting point of the oxide (1159 K). As seen from the figure, the data reported in literature are in agreement with each other within ±2 kJ. The present data are in excellent agreement throughout the temperature range with those of Knacke et al. [9], Chase et al. [10], Jacobs and Jeffes [14] and Bannister [22]. Data which show significant difference in the entire temperature region of investigation are those reported by Mehrotra et al. [16] and Iwase et al. [18]. Data reported by Sugimoto et al. [21] and Charette and Flengas [13] are in good agreement at high temperatures while significant deviations are seen at lower temperatures. The data reported by Szwarc et al. [15], Charle and Osterwald [19], Taskinen [20], Mehrotra et al. [16] and Mallika and Sreedharan [23] were based on measurements carried out in small ranges of temperature only (148°, 121°, 73°, 166° and 134°, respectively).

Data reported by Jacobs and Jeffes [14], Iwase et al. [18] and Alcock and Belford [11] were from emf measurements using CSZ based cells with Ni/NiO reference

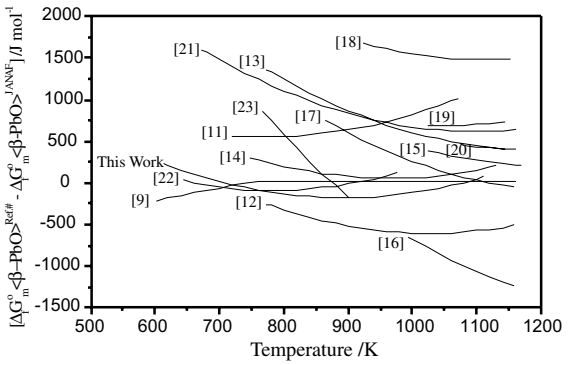

Fig. 4. Difference between experimental values and JANAF data on $\Delta_f G^0_m\langle\beta\text{-PbO}\rangle$ as a function of temperature.

electrode system. A close examination of the emf data by Jacobs and Jeffes, and Iwase et al. showed excellent agreement between them. Jacobs and Jeffes derived $\Delta_f G^0_m\langle\text{PbO}\rangle$ values from their emf data using the $\Delta_f G^0_m\langle\text{NiO}\rangle$ data reported by Steele [29]. Iwase et al. had used $\Delta_f G^0_m\langle\text{NiO}\rangle$ data obtained from an auxiliary cell employed by them. The significant deviation in $\Delta_f G^0_m\langle\text{PbO}\rangle$ reported by Iwase et al. is thus clearly arising from thermochemical data on $\Delta_f G^0_m\langle\text{NiO}\rangle$ used by them. Similarly, a small deviation observed in the data reported by Alcock and Belford [11], particularly at high temperatures could be traced to the values of $\Delta_f G^0_m\langle\text{NiO}\rangle$ employed by them. The authors had derived $\Delta_f G^0_m\langle\text{NiO}\rangle$ from gas equilibration experiments for this purpose [11]. $\Delta_f G^0_m\langle\text{PbO}\rangle$ derived from their emf data by employing $\Delta_f G^0_m\langle\text{NiO}\rangle$ values reported by Steele [29] showed very good agreement with the present data and those of Jacobs and Jeffes [14] at all temperatures.

Choice of electrical lead for use with Pb/PbO electrode had always been a critical factor because of the corrosive nature of Pb. Based on chemical compatibility considerations, iridium had been used as electrical lead for the Pb/PbO electrode system by majority of the investigators. However, Mehrotra et al. [16] had used stainless steel as the electrical lead. The components of stainless steel are soluble in liquid Pb [3] and compounds of Pb–M–O (M: Fe, Cr, Mn) are known in the literature [30]. The differences observed between the present work and those of Mehrotra et al. [16] could be due to these chemical interactions of stainless steel electrical lead with Pb/PbO electrode system. Platinum was used as electrical lead for Pb/PbO electrode by Matsushita and Goto [12]. It is known that platinum is not compatible with lead as it forms intermetallic compounds with Pb and forms eutectic in Pb rich region [3]. $Cr–Al_2O_3$ cermet was used as electrical lead for Pb/PbO electrode system by Jacobs and Jeffes [14], Taskinen [20] and Bannister [22]. Jacob and Jeffes had observed the attack of the cermet by the Pb/PbO system particularly close to the melting point of PbO (1159 K) and hence resorted to Ir as electrical lead. Bannister had used $Cr–Al_2O_3$ cermet tube as container as well as electrical lead of Pb/PbO electrode system. Since the highest temperature of that investigation was only 977 K, problems due to incompatibilities could have been less significant though this could be a concern in the investigations by Taskinen since the temperature range of investigation in that work was between 1073 and 1145 K. Mallika and Sreedharan [23] had used a graphite cup to contain the Pb–PbO electrode and for the protection of platinum electrical lead. PbO is reduced by graphite to Pb and this can be a problem particularly while operating the cells at high temperatures. Though the authors had restricted their highest temperature to 901 K, a small but distinct temperature dependent deviation of their data from the present values is seen. The reasons for the deviations of the data reported by Charette and Flengas [13] and Sugimoto [21], particularly at low temperatures are not clear but existence of non-equilibrium conditions during their investigations at these temperatures is a distinct possibility.

Risold et al. [8] has reported the optimised values of Gibbs free energy of formation of PbO(s) and this was based on all the thermochemical data of PbO(s) available in literature with a higher weightage given to data derived from emf studies. However, during this optimisation no discriminations were made among the reported works and many of the above-mentioned experimental parameters in the emf investigations were not taken into account. Hence the optimised values reported by Risold et al. were not used for comparison with the present results.

The data reported in the present work are considered to be very reliable since this involved a large number of equilibrium measurements over a wide range of temperature and were carried out after extended periods of equilibration. Measurements could be extended to temperatures close to the melting point of lead using RuO_2 as electrode material with O_2 gas as reference.

Acknowledgements

The authors acknowledge Dr G. Periaswami, Head, Materials Chemistry Division, IGCAR for his constant encouragement during this work. The authors also acknowledge Dr R. Viswanathan, Materials Chemistry Division and Dr V. Venugopal, Head, Fuel Chemistry Division, BARC for helpful discussions.

References

[1] B.F. Gromov (Ed.), Heavy Liquid Metal Coolants in Nuclear Technology (HLMC-98), Vols. 1 and 2, SSC RF-IPPE, Obninsk, 1999.

[2] H.U. Borgstedt, C.K. Mathews, Applied Chemistry of Alkali Metals, Plenum, New York and London, 1987.
[3] T.B. Massalski (Ed.), Binary Alloys Phase Diagrams, The Materials Information Society, USA, 1990.
[4] B.F. Gromov, G.I. Toshinsky, V.V. Checkunov, Y.I. Orlov, Y.S. Belomytsev, I.N. Gorelov, A.G. Karabash, M.P. Leonchuk, D.V. Pankratov, Y.G. Pashkin, in: B.F. Gromov (Ed.), Heavy Liquid Metal Coolants in Nuclear Technology (HLMC-98), Vol. 1, SSC RF-IPPE, Obninsk, 1999, p. 14.
[5] N. Li, J. Nucl. Mater. 300 (2002) 73.
[6] P.N. Martynov, Y.I. Orlov, in: B.F. Gromov (Ed.), Heavy Liquid Metal Coolants in Nuclear Technology (HLMC-98), Vol. 2, SSC RF-IPPE, Obninsk, 1999, p. 565.
[7] H.A. Wriedt, Bull. Alloy Phase Diagrams 9 (1988) 106.
[8] D. Risold, J.-I. Nagata, R.O. Suzuki, J. Phase Equilibria 19 (1998) 213.
[9] O. Knacke, O. Kubaschewski, K. Hesselmann (Eds.), Themochemical Properties of Inorganic Substances, Vol. 2, Springer, Berlin, 1991, p. 1559.
[10] M.W. Chase Jr., C.A. Davies, J.R. Downey Jr., D.J. Frurip, R.A. McDonald, A.N. Syverund (Eds.), JANAF Thermochemical Tables, 3rd Ed., Part II, American Institute of Physics, NBS, New York, 1985, p. 1644.
[11] C.B. Alcock, T.N. Belford, Trans. Faraday Soc 60 (1964) 822.
[12] Y. Matsushita, K. Goto, in: Thermodynamics, Vol. 1, IAEA, Vienna, 1966, p. 111.
[13] G.G. Charette, S.N. Flengas, J. Elctrochem. Soc 115 (1968) 796.
[14] K.T. Jacob, J.H.E. Jeffes, Trans. Inst. Min. Metall. 80 (1971) C32.
[15] R. Szwarc, K.E. Oberg, R.A. Rapp, High Temp. Sci. 4 (1972) 347.
[16] G.M. Mehrotra, M.G. Frohberg, P.M. Mathew, M.L. Kapoor, Scr. Metall. 7 (1973) 1047.
[17] W.F. Caley, C.R. Masson, in: Z.A. Foroulis, W.W. Smelzer (Eds.), Metal-Slag-Gas Reactions and Processes, The Electrochemical Soc, New Jersey, 1975, p. 140, cited from [7].
[18] M. Iwase, K. Fujimura, T. Mori, Trans. JIM 19 (1978) 377.
[19] H. Charle, J. Osterwald, Z. Phys. Chem. NF 99 (1976) 199.
[20] A. Taskinen, Scand. J. Metall. 8 (1979) 185.
[21] E. Sugimoto, S. Kuwata, Z. Kozuka, J. Jpn. Inst. Met. 44 (1980) 644, cited from [7] and [21].
[22] M.J. Bannister, J. Chem. Themodyn. 16 (1984) 787.
[23] C. Mallika, O.M. Sreedharan, Mat. Lett. 22 (1995) 5.
[24] C. Mallika, O.M. Sreedharan, R. Subasri, J. Euro. Cer. Soc. 20 (2000) 2297.
[25] S.P.S. Badwal, F.T. Ciacchi, J. Appl. Electrochem. 16 (1986) 28.
[26] K. Kunstler, H.-J. Lang, W. Richter, P. Shuk, Diffus. Defect Data, Part B 39&40 (1994) 255.
[27] G. Periaswami, S. Vana Varamban, S. Rajan Babu, C.K. Mathews, Solid State Ion. 26 (1988) 311.
[28] W.B. White, F. Dachille, R. Roy, J. Am. Ceram. Soc. 44 (1961) 170.
[29] B.C.H. Steele, in: C.B. Alcock (Ed.), Electromotive Force Measurements in High Temperature Systems, Institution of Mining and Metallurgy, London, 1968, p. 3.
[30] R.S. Roth, J.R. Dennis, H.F. McMurdie (Eds.), Phase Diagrams for Ceramists, Vol. IV, The American Ceramic Society, Ohio, 1987.